The conversion of methane with silica-supported platinum catalysts: the effect of catalyst preparation method and platinum particle size

M. Eswaramoorthy, S. Niwa, M. Toba, H. Shimada, A. Raj and F. Mizukami *

National Institute of Materials and Chemical Research, 1-1 Higashi, 305-8565 Ibaraki, Japan

Received 18 July 2000; accepted 31 October 2000

The particle size distribution of platinum in silica prepared by the complexing agent-assisted sol–gel method and impregnation method and also in MCM-41 has been compared and its influence on the product distribution in the non-oxidative dehydrogenation of methane has been investigated. The sol–gel method gives a narrow range of platinum particle size distribution compared to the impregnation method. It was found that as the particle size increases, the selectivity for the higher hydrocarbons increases though the yield decreases.

KEY WORDS: methane; non-oxidative dehydrogenation; mesoporous; Pt-silica

1. Introduction

Efforts are being made to convert methane, which is considered to be a clean fuel, into higher hydrocarbons for the past two decades [1]. The strong equivalent C–H bonds, absence of polarity and absence of functional groups make chemical conversion of methane to liquid hydrocarbons an energy intensive process [2]. Three ways are mainly explored for the conversion of methane to higher hydrocarbons [3,4]. One is an indirect way in which methane is first converted to syngas by steam or CO_2 reforming or through partial oxidation [5] and the resultant syngas is further converted to higher hydrocarbons. Another way is an oxidative dehydrogenation (OCM process) where the conversion is high, but part of the methane gets converted to undesired CO_2 and hence reduces the selectivity of the reaction [6–9]. The third one is a non-oxidative dehydrogenation which gains momentum in recent years, since it avoids the complete combustion and higher operating temperature (>973 K) associated with the oxidative coupling reaction, but still the conversion is very low.

In order to circumvent the thermodynamic problems, the non-oxidative reaction is usually carried out in two steps at different temperatures, the first being the activation of methane over the metal surface at higher temperature and then hydrogenation of the carbonaceous deposits at lower temperature [10]. Nevertheless, activation of methane and the subsequent hydrogenation at the same temperature were also reported [11–18].

Transition metals are known for the decomposition of methane but their strong bonding to the carbonaceous species makes their reactivity very low and paves the way for the noble metals, whose interaction with carbonaceous species is weaker [11]. Among the noble metals platinum in an inert support is widely being used for the activation of methane. Many parameters such as flow rate of methane, temperature of activation, reactant pressure, aging time, hydrogen flow rate, hydrogenation temperature, and nature of support have direct bearings on the product distribution since they are known to have an influence on the C–C bond homologation over the same catalyst [10,19–27]. Trevor et al. [28] reported that the activation of methane over Pt clusters is size selective. Indeed, platinum supported on silica on exposure to methane is known to give CH_x species, which on subsequent hydrogenation gives higher hydrocarbons. However, the effect of Pt particle size and the preparation method on the distribution of products in the non-oxidative coupling of methane is not well known. Complexing agent-assisted sol–gel synthesis is envisaged to obtain platinum of desired particle size on a silica support with uniform distribution. In this paper we report the effect of platinum in silica prepared by sol–gel as well as impregnation methods and also in MCM-41 on the products selectivity in the non-oxidative dehydrogenation of methane.

2. Experimental

2.1. Preparation of Pt–SiO_2 by the sol–gel technique

In a typical manner, a required amount (1, 5 and 6.3 wt% of platinum with respect to silica) of platinum as $Pt(NO_2)_2(NH_3)_2$ was mixed with excess ethylene glycol of about 100 ml along with acetylacetone keeping the ratio Pt/acac equal to 0.008. The mixture was heated at 363 K for 2 h to obtain a clear solution. To this a required amount of tetraethyl orthosilicate (TEOS) mixed with equal amount of ethanol was added and this mixture was again stirred at the same temperature for 4 h. After that water (TEOS/$H_2O = 0.25$) with the same amount of ethanol was added to hydrolyse the TEOS. The above solution was allowed to stir overnight at the same temperature to get the transparent gel.

* To whom correspondence should be addressed.

This was dried in vacuum to remove the solvent by slowly raising the temperature from 333 to 393 K. Then it was powdered and calcined at 773 K for 10 h and subsequently reduced with hydrogen at 673 K for 8 h.

Pure silica was also prepared by the same method except adding the platinum precursor with acetyl acetone. This was calcined at 773 K for 10 h and then impregnated with 6.3 wt% Pt using dinitrodiammino-Pt(IV) precursor. It was further reduced with hydrogen at 673 K for 8 h. The Pt-silicas prepared by sol–gel and impregnation methods are designated as Pt-silica (SG) and Pt-silica (imp), respectively.

2.2. Preparation of Pt-MCM-41

3 g of cetyltrimethylammonium bromide was dissolved in 50 ml of water. To this 2.8 ml of 5 M NaOH solution was added followed by 0.2 g of platinic ammonium chloride and stirring for 1 h. Then 6.2 ml of TEOS was added slowly with stirring. This gel was stirred further 2 h and allowed standing at room temperature for five days. After that it was filtered and washed with deionised water and dried at 383 K for 5 h before calcining it at 773 K in air for 10 h followed by reduction at 673 K with hydrogen for 5 h. In addition, platinum (6.3 wt%) was incorporated in uncalcined MCM-41 by impregnation and then calcined at 773 K in air for 10 h and reduced with hydrogen at 673 K for 5 h. The same amount of platinum was impregnated over calcined MCM-41 and then reduced in hydrogen atmosphere at 673 K for 5 h. These catalysts are designated as 6.3% Pt-MCM-41 (SG), 6.3% Pt-MCM-41 (brt) and 6.3% Pt-MCM-41 (art), respectively, where "brt" and "art" stand for before and after removing the template, respectively.

2.3. Sample characterisation

The platinum content was estimated using an X-ray fluorescence spectrometer (SEIKO SEA-2010). Thermogravimetric analyses of the calcined samples were carried out on a MAC Science TG-DTA 2100 instrument in dry air (100 ml/min) with the heating rate 10 K/min. For other measurements only reduced samples were used. Hydrogen and CO chemisorptions were carried out at room temperature using a quartz U-tube reactor fitted with a TCD detector. For the chemisorption experiment, 50 mg of the sample was pretreated at 573 K in hydrogen for 1 h and then brought to room temperature with a flow of Ar/He for hydrogen/CO chemisorption, respectively. The surface area was determined by the BET method [29] at liquid-nitrogen temperature using a Belsorp-2000 instrument. The adsorption–desorption isotherm was also obtained by using nitrogen as the adsorbate. The pore size of 6.3% Pt-MCM-41 (SG) was calculated using the Dollimore–Heal (DH) model [30]. The transmission electron microscope (TEM) measurement was done by using Jeol-FX-2000 equipment. X-ray photoelectron spectroscopy (XPS) measurements were performed with a Perkin–Elmer ESCA5500 X-ray photoelectron spectrometer using Mg K_α excitation source. The binding energies were normalised with respect to the C(1s) line at 285 eV.

2.4. Non-oxidative dehydrogenation of methane

All the reactions were carried out using a stainless-steel reactor connected with an on-line gas chromatograph. 0.4 g of catalyst was heated under helium stream at the reaction temperature for 1 h at 573 K before carrying out the reaction. Then methane diluted with helium in the ratio 3 : 10 (v/v) was introduced for 5 min. After that the gas was immediately switched over to hydrogen at the same temperature with the flow rate of 20 ml/min and the products were collected for 1 h in a sample loop kept at liquid-nitrogen temperature. The trapped products were analysed by heating the loop at 573 K and injected as a whole into the Shimadzu GC14B equipped with a Supel-Q PLOT column and the FID detector.

3. Results and discussion

The adsorption isotherms results from the physical adsorption were classified into type I to type V by Brunauer, Deming, Deming and Teller [31]. Samples having micropores (pore size <2 nm), like zeolites, are known to exhibit type I isotherms. Adsorption on non-porous solids gives type II isotherm. Solids with microporosity and significant external surface are known to give type II isotherms which is a merger of type I, a steep rise at lower region of p/p_0, and type II [32]. The presence of micropore volume can be identified using the t-plot analysis. This is based on

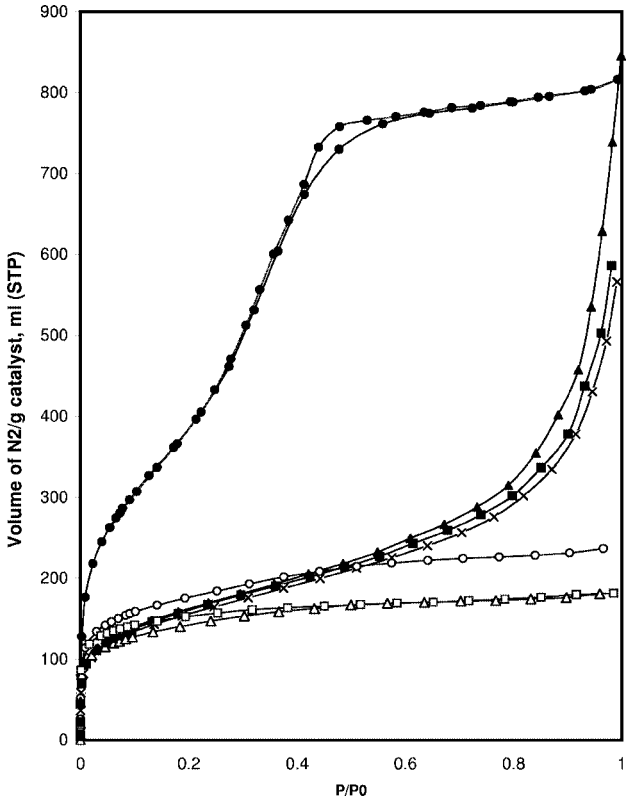

Figure 1. Nitrogen adsorption isotherms. (●) 6.3% Pt-MCM-41 (SG), (▲) 6.3% Pt-silica (imp), (■) 5% Pt-silica (imp), (×) silica, (○) 1% Pt-silica (SG), (□) 5% Pt-silica (SG) and (△) 6.3% Pt-silica (SG).

the t-curve, a plot of the standard isotherm with t, the statistical thickness of the film [33]. Solids having the pore size in the mesoporous range will show type IV isotherm. The nitrogen adsorption isotherms of all Pt-silica samples prepared by the sol–gel method in this study exhibit type I isotherm indicating the presence of micropores, shown in figure 1. However, pure silica prepared by the sol–gel method and the Pt-silica (imp) depict type-II isotherm, also including type I in the lower p/p_0 region. The t-plot analysis confirmed the presence of micropores. The surface area of silica and all the platinum-incorporated silicas are in the range of 500–600 m^2/g (table 1). The surface area of Pt-silica (SG) decreases from 640 m^2/g for 1% Pt loading to 514 m^2/g for 6.3% Pt loading. However, the surface area of Pt-silicas (imp) is more or less the same as that of pure silica. The 6.3% Pt-MCM-41 (SG) gives very high surface area of 1440 m^2/g.

The 6.3% Pt-MCM-41 (SG) shows type-IV isotherm typical for mesoporous material with the hysteresis in the higher p/p_0 region (figure 1). The pore size calculated by the DH-model is found to be 3 nm in diameter (figure 2). The XRD pattern (not included) of the samples before and after calcination shows the peaks typical for hexagonal structure.

From the TG analysis it was confirmed that all the calcined samples are free of any templates. Figure 3 presents the histograms of particle size distribution obtained by the TEM analysis. It shows that the Pt particle size increases with increase of metal loading and shows a narrow range of distribution for the catalysts prepared by the sol–gel method. A wide range of distribution is observed for the Pt-silica prepared by the impregnation method. Moreover, the par-

Table 1
Surface area and chemisorption data.

Catalyst	CO/Pt	H/Pt	Surface area (m^2/g)
1% Pt-silica (SG)	0.184	0.147	640
5% Pt-silica (SG)	0.189	0.171	564
6.3% Pt-silica (SG)	0.131	0.129	514
6.3% Pt-MCM-41 (SG)	0.044	0.023	1440
5% Pt-silica (imp)	0.038	0.012	556
6.3% Pt-silica (imp)	0.042	0.025	584
Silica	–	–	583

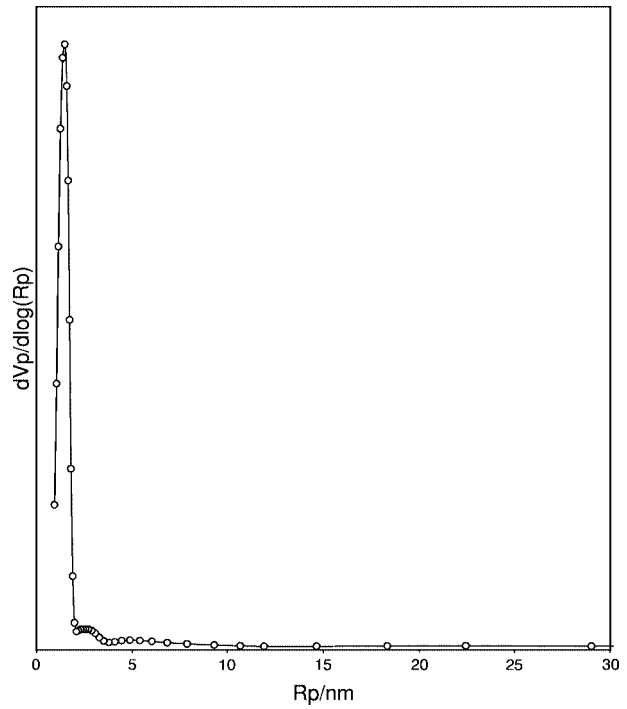

Figure 2. Pore size distribution of 6.3% Pt-MCM-41 (SG) after removing the surfactant.

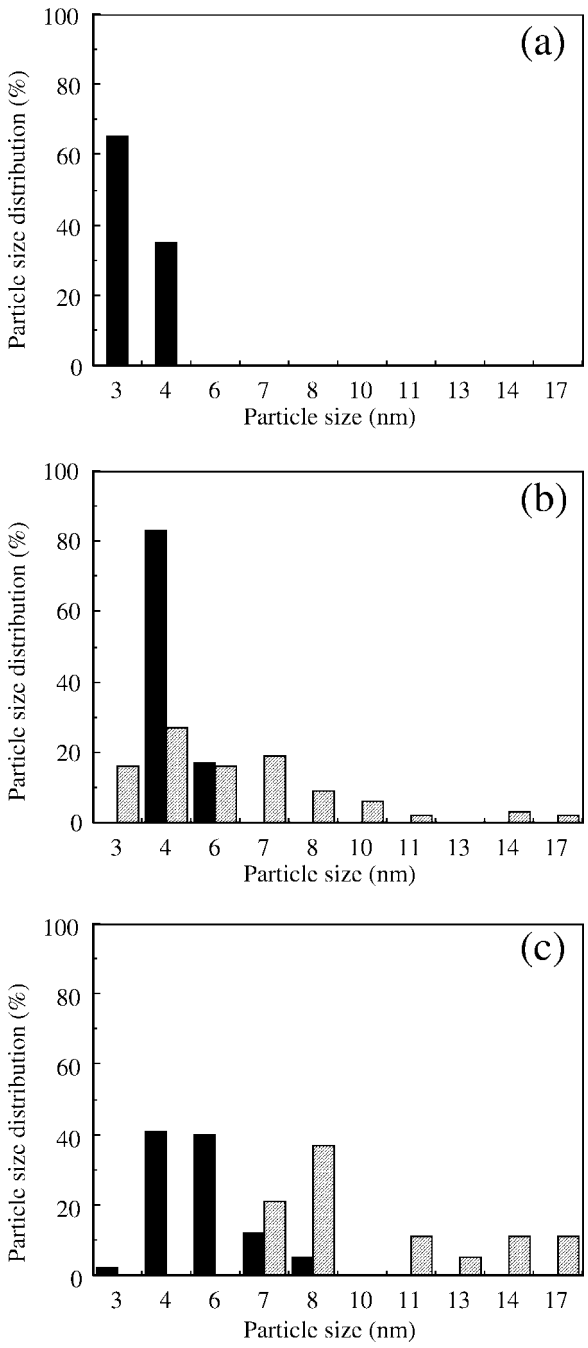

Figure 3. Particle size distribution of platinum over (a) 1% Pt-silica (SG), (b) 5% Pt-silica, (c) 6.3% Pt-silica ((■) sol–gel and (□) impregnation).

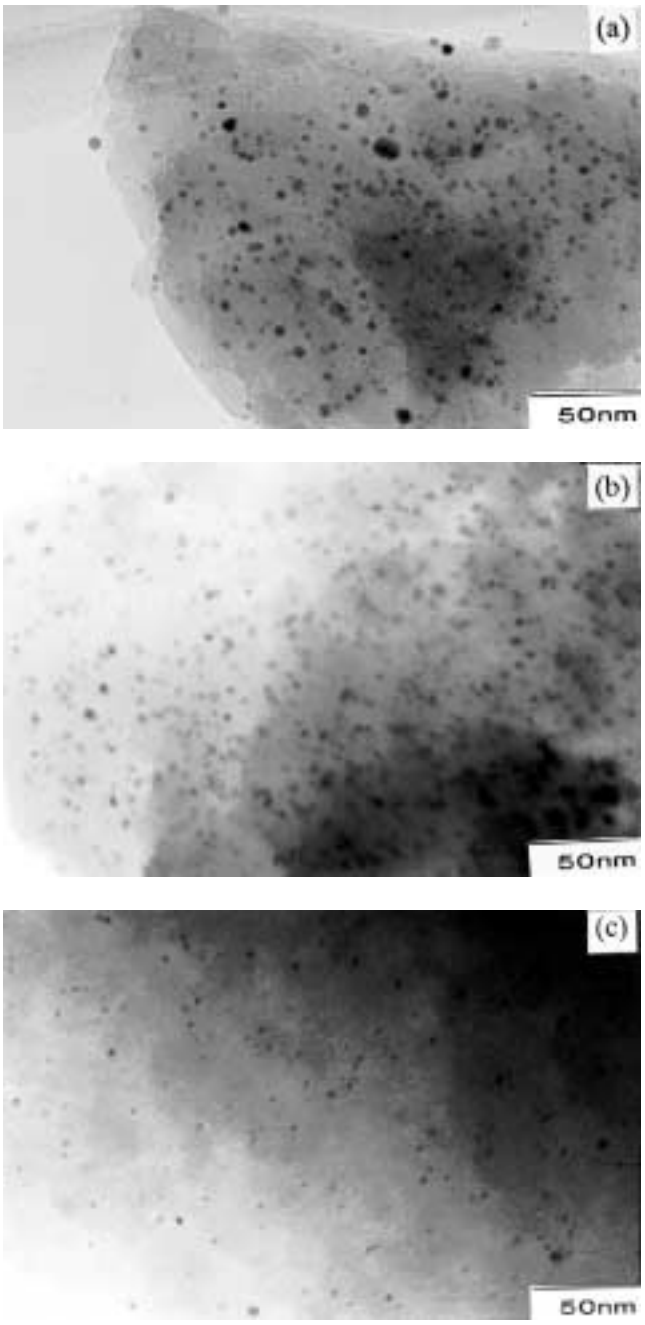

Figure 4. TEM images of (a) 5% Pt-silica (imp), (b) 5% Pt-silica (SG) and (c) 1% Pt-silica (SG).

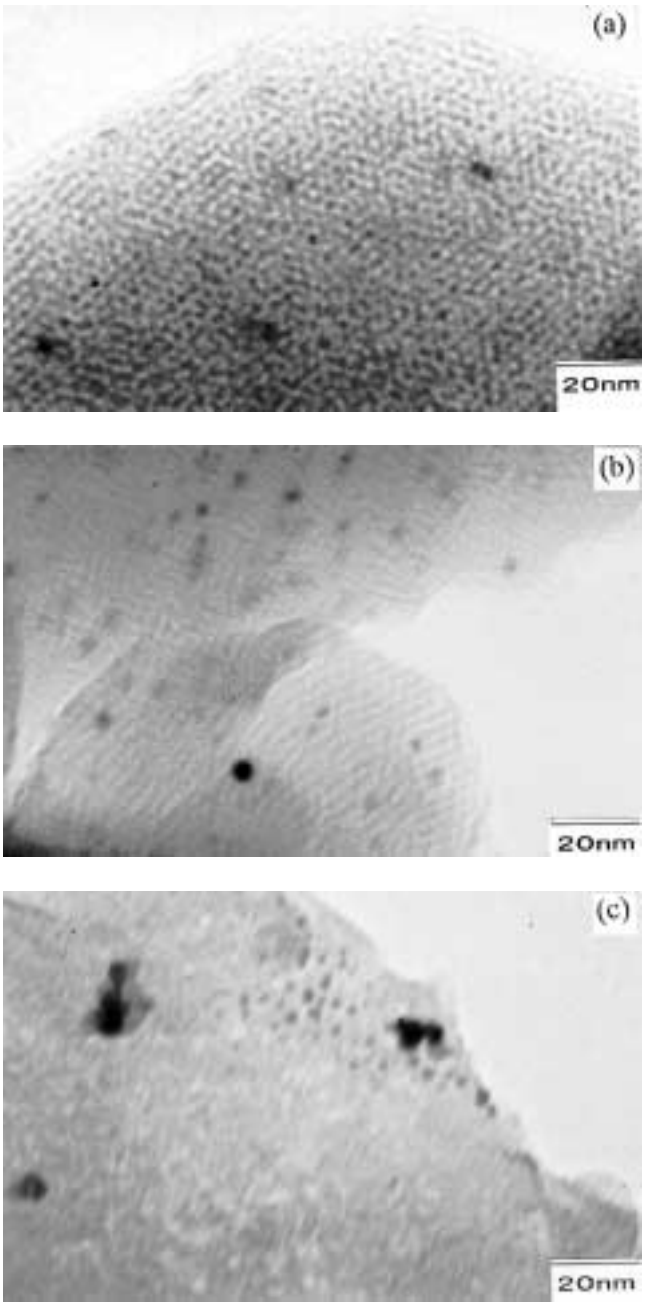

Figure 5. TEM images of (a) 6.3% Pt-MCM-41 (SG), (b) 6.3% Pt-MCM-41 (brt) and (c) 6.3% Pt-MCM-41 (art).

ticle size of platinum at the same loading is comparatively higher for the impregnated Pt-silica than for the one prepared by the sol–gel method (figure 4). In the case of 6.3% Pt-MCM-41 (SG) the distribution is maximum around 3–5 nm (figure 5(a)) and 75% of the Pt particles are in the range of 3 nm size.

The chemisorption of all the Pt-silicas prepared by the sol–gel method is significantly higher than the Pt-silica impregnated samples as well as 6.3% Pt-MCM-41 (SG) (table 1). In all the cases the CO uptake is higher than the hydrogen uptake. TEM analyses (figure 3) show that the particle size of platinum obtained by the impregnated method is bigger than the sol–gel one and this might be the reason for the lower amount of hydrogen and CO chemisorption. In the case of 6.3% Pt-MCM-41 (SG), the hydrogen and CO uptake are similar to those of Pt-silica (imp) catalysts, even though the particle size observed by TEM is maximum around 3–5 nm. This lower amount of hydrogen and CO uptake could be attributed to metal–support interaction similar to the one reported in the literature for the Co on silica support [34–37]. From table 2 it is observed that the amount of carbon formed over the catalysts in the first step, methane activation, increases in the following order 6.3% Pt-MCM-41 (SG) < 5% Pt-silica (SG) < 5% Pt-silica (imp), whereas the binding energy of Pt^0 and the conversion of the carbona-

ceous species into C_2–C_6 products follow the reverse order, 5% Pt-silica (imp) < 5% Pt-silica (SG) < 6.3% Pt-MCM-41 (SG). It seems that activation of methane is less pronounced when the electron deficiency of platinum is more. In 6.3% Pt-MCM-41 (SG), the large surface area of MCM-41, and small Pt particle size favours the higher metal–support interfacial area, which results in comparatively higher intensity of metal–support interaction. Since methane is a weak acid, its adsorption will be more favoured on electron-rich platinum. The decrease in electron density in platinum could be attributed to the above order in the carbon formation observed in our study. Amariglio and co-workers [38] reported that adsorption of methane over Pt on HY support was lower than on HX where the Pt in the former is more electron deficient than the latter.

However, it is important to note that all the carbon formed in the first step, activation of methane, is not getting converted into the products on subsequent hydrogenation. It further depends on the type, amount, thermal history and age of carbonaceous species formed [39,40]. Van Santen et al. [10] classified the carbon formed during the activation of methane over the transition metal supported catalysts into three types, namely C_α, C_β and C_γ, based on their reactivity towards hydrogenation. Of these, only C_α, the active carbonaceous species, is known to give C_2 and other hydrocarbons on hydrogenation. The other two types give mainly methane on hydrogenation. Bell and co-workers [41,42] showed, based on a ^{13}C study, that C_α is composed of single carbon atoms, C_β is composed of C_yH_x species, and C_γ is composed of graphitic carbon. They further classified C_α, into $C_{\alpha1}$ and $C_{\alpha2}$, and C_β into $C_{\beta1}$, $C_{\beta2}$ and $C_{\beta3}$ based on TPSR studies of the coke formed over Ru/SiO_2 [27]. Moreover, C_α and C_β, which are in dynamic equilibrium, slowly transformed to unreactive graphitic, type carbon C_γ, on aging, which is an irreversible process. In a similar way Marceau et al. [43] classified the surface carbonaceous species on ruthenium into C_α (C_2 units), $C_{\beta1}$ (lighter species) and $C_{\beta2}$ (heaviest and most inert species). They observed that the heavier fraction, $C_{\beta2}$, on slow hydrogenolysis leads to C_6–C_8 production, depending on the history of the catalyst and the behaviour of its "graphitic" reservoir.

Table 2
XPS data and the total amount of carbon deposited in the conversion of methane at 573 K.

Catalyst	Total amount of carbon[a] estimated as CO_2 (μmol)	Binding energy of Pt^0 (eV)
5% $Pt–SiO_2$ (imp)	47.0	71.02
5% $Pt–SiO_2$ (SG)	31.2	71.27
6.3% Pt-MCM-41 (SG)	13.8	71.40

[a] Total amount of carbon deposited on the surface of the catalyst after passing the methane and helium (3 : 10 v/v) mixture for 5 min at 573 K was estimated as CO_2 by passing oxygen at 623 K for 20 min and the trapped CO_2 was analysed using a GC equipped with TCD detector.

Table 3 gives the product distribution in the conversion of methane over the catalyst at 573 K. The total amount of products formed over Pt-silica prepared by the sol–gel method is higher than over the Pt-silica impregnated catalysts. 6.3% Pt-MCM-41 (SG) exhibits higher activity among all the catalysts. The selectivity for C_2 products over 1, 5 and 6.3% Pt-silica prepared by the sol–gel method is higher compared to C_{6+} (includes hexane, benzene and toluene) products, as shown in figure 6(a). Moreover, the C_{6+} selectivity shows an increasing trend with respect to increase in metal loading or, in other words, with increase in particle size. The higher selectivity for C_2 hydrocarbons over Pt-silica (SG) could be explained on the basis that the Pt particles trapped inside the silica matrix, could have exposed partly to the walls of micropores where CH_4 becomes dehydrogenated to CH_x species, and then converted to mainly C_2 hydrocarbons on further hydrogenation. The absence of any significant amount of meso- or macropores in the Pt-silica (SG) shown by the nitrogen adsorption isotherm (type I) combined with the uniform platinum particle size distribution clearly indicates that the Pt particles might be trapped inside the silica matrix during the sol–gel process and further calcination leaves micropores due to the removal of the solvent ethylene glycol. Since the particle size of Pt in all the catalysts is above 2 nm, as observed by TEM, there is a possibility that these particles could not be exposed fully into the micropores and the extent of exposure depends on the size of the Pt particle. As a result, the propagation of adsorbed CH_x species leading to higher hydrocarbons is reduced. Whereas in the case of impregnated catalysts, exhibiting type-II isotherms similar to pure silica for the presence of macropores (or flat surface), the Pt

Table 3
Products distribution in methane conversion over the catalysts.

Catalyst	C_2 (μmol)	C_3 (μmol)	C_4 (μmol)	C_5 (μmol)	C_6 (μmol)	Total amount of products (μmol)	Amount of products in terms of carbon (μmol)
1% Pt-silica (SG)	0.080	0.028	0.005	0.015	0.008	0.136	0.380
5% Pt-silica (SG)	0.265	0.025	0.010	0.018	0.025	0.343	0.880
6.3% Pt-silica (SG)	0.159	0.032	0.009	0.024	0.032	0.256	0.750
6.3% Pt-MCM-41 (SG)	0.276	0.048	0.016	0.040	0.028	0.408	1.200
5% Pt-silica (imp)	0.031	0.012	0.007	0.006	0.012	0.068	0.227
6.3% Pt-silica (imp)	0.031	0.017	0.010	0.010	0.016	0.083	0.300

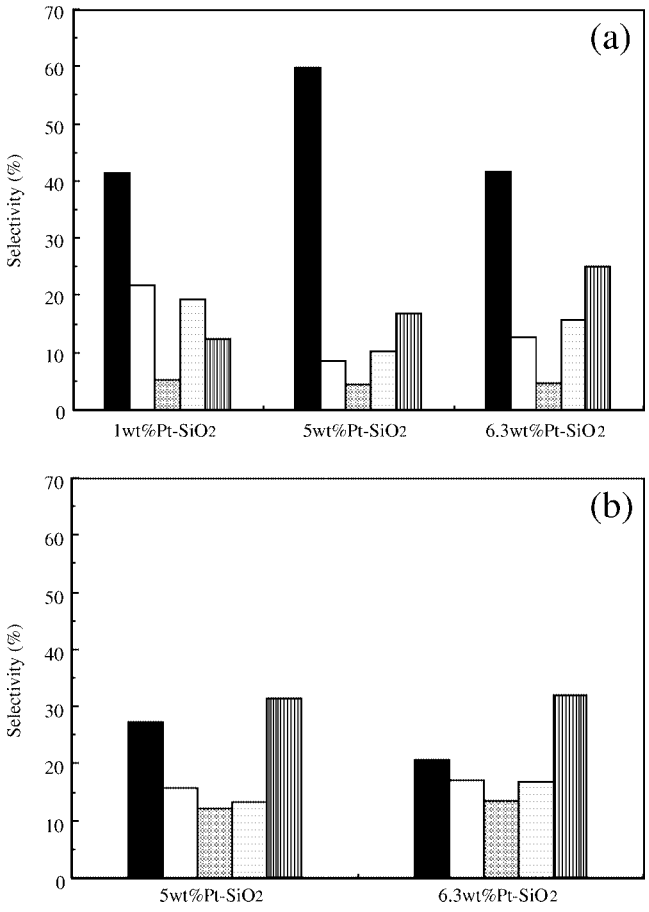

Figure 6. Effect of Pt content on the selectivity of products in methane conversion (a) sol–gel and (b) impregnation. (■) C_2, (□) C_3, (▨) C_4, (▭) C_5 and (▥) C_6.

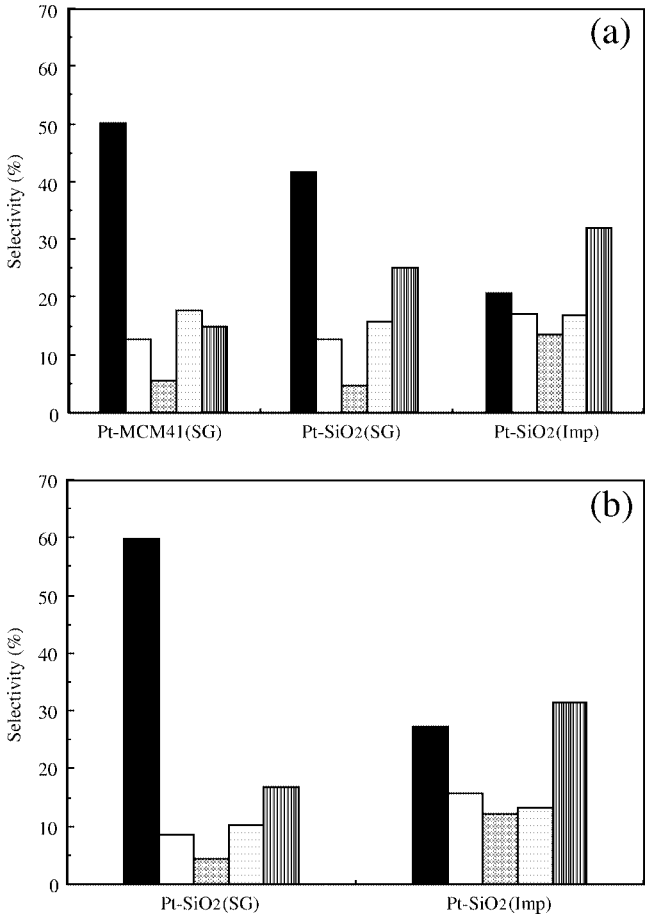

Figure 7. Effect of preparation methods on the selectivity of products in methane conversion (a) 6.3% Pt-silica and (b) 5% Pt-silica. (■) C_2, (□) C_3, (▨) C_4, (▭) C_5 and (▥) C_6.

Table 4
Products selectivity (on the carbon basis) over Pt-MCM-41 catalysts in the conversion of methane.

Catalyst	Selectivity (%)					Total amount of products (μmol/g)
	C_2	C_3	C_4	C_5	C_6	
6.3% Pt-MCM-41 (SG)	50.06	12.75	5.60	17.70	14.89	1.20
6.3% Pt-MCM-41 (brt)	24.20	39.50	0.60	7.30	28.20	1.17
6.3% Pt-MCM-41 (art)	35.10	37.80	–	–	27.00	1.20

particles should be present mostly on the macropores or on the silica surface where the dehydrogenated CH_x species can undergo further condensation leading to heaviest species (like $C_{\beta 2}$) without any hindrance which on hydrogenolysis results in higher selectivity for C_{6+} hydrocarbons (figure 6(b)).

Figure 7(a) compares the product distribution over 6.3% Pt-MCM-41 (SG), 6.3% Pt-silica (sol–gel) and 6.3% Pt-silica (imp) in the non-oxidative dehydrogenation of methane. As the particle size increases, the distribution of C_{6+} products also increases and at the same time C_2 formation is getting reduced. The comparatively higher and lower selectivity for C_2 and C_{6+} hydrocarbons, respectively, over 6.3 Pt-MCM-41 (SG) might be explained both in terms of smaller particle size as well as metal–support interaction. The same trend occurs between 5% Pt-silica (SG) and 5% Pt-silica (imp) shown in figure 7(b).

In order to find out the effect of platinum only outside and also both outside and inside the mesopores, we have introduced platinum into both uncalcined and calcined MCM-41. The TEM picture (figure 4) shows that platinum is incorporated both inside and outside the mesopores in 6.3% Pt-MCM-41 (art) and the incorporation is mostly restricted to outside the pores in 6.3% Pt-MCM-41 (brt). The fact that the particle size is comparatively uniform in the latter than in the former might be due to the effect of template.

Table 4 compares the product distribution over 6.3% Pt-MCM-41 (SG), 6.3% Pt-MCM-41 (art) and 6.3% Pt-MCM-

41 (brt) catalysts. The total amount of products formed over all the three catalysts is more or less the same but the distribution of products is quite different. The amounts of C_3 and C_{6+} products are larger over 6.3% Pt-MCM-41 (art) and 6.3% Pt-MCM-41 (brt) than over 6.3% Pt-MCM-41 (SG) which exhibits higher amount of C_2 formation. This can be reasoned out to the difference in particle size distribution.

4. Conclusion

The selectivity for the C_{6+} hydrocarbons in the methane conversion over platinum silica prepared by the impregnation method is more as compared to the sol–gel method whose particle size is small and the size distribution is uniform. The activation of methane is more pronounced over the impregnated catalyst than over the sol–gel catalysts which results in higher amount of coke formation in the first step. This might be due to the higher electron density associated with the Pt in the former than in the latter. The bigger Pt particles and their free access on the surface of silica over the impregnated catalyst favour the condensation of CH_x species, which might lead to heaviest carbonaceous species. This on hydrogenolysis results in a higher selectivity for C_{6+} hydrocarbons. The smaller and uniform Pt particle size distribution and their accessibility through the micropores over the sol–gel catalysts reduces the chance for the formation of heaviest carbonaceous species and hence enhances the selectivity for C_2 hydrocarbons.

Acknowledgement

ME is indebted to Science and Technology Agency (STA), Japan for financial support.

References

[1] Y. Ono, in: *Methane Conversion*, eds. D.M. Bibby, C.D. Chang, R.F. Howe and S. Yurchak, Catal. Rev. Sci. Eng. 34 (1992) 179.
[2] D.M. Golden and S.W. Benson, Chem. Rev. 69 (1969) 125.
[3] K. Fujimoto, Stud. Surf. Sci. Catal. 81 (1994) 7.
[4] J.R. Rostrup-Nielsen, Catal. Today 21 (1994) 257.
[5] A.T. Ashcroft, A.K. Cheetham, J.S. Foord, M.L.H. Green, C.P. Grey, A.J. Murrell and D.F. Vernon, Nature 344 (1990) 319.
[6] T. Ito and J.H. Lunsford, Nature 314 (1985) 721.
[7] G.E. Keller and M.M. Bhasin, J. Catal. 73 (1982) 9.
[8] T. Ito, J.-X. Wang, C.H. Lin and J.H. Lunsford, J. Am. Chem. Soc. 107 (1985) 5062.
[9] J.A. Sofranko, J.J. Leonard and C.A. Jones, J. Catal. 103 (1987) 302.
[10] T. Koerts, M.J.A. Deelen and R.A. van Santen, J. Catal. 138 (1992) 101.
[11] L. Guczi, R.A. van Santen and K.V. Sarma, Catal. Rev. Sci. Eng. 38 (1996) 249.
[12] L. Guczi, G. Stefler, Zs. Koppany, L. Borko, S. Niwa and F. Mizukami, App. Catal. A 3939 (1997) 1.
[13] J.S.M. Zadeh and K.J. Smith, J. Catal. 183 (1999) 232.
[14] T. Koerts and R.A. van Santen, J. Chem. Soc. Chem. Commun. (1991) 1281.
[15] E. Marceau, J.M. Tatibouet, M. Che and J. Saint-Just, J. Catal. 183 (1999) 384.
[16] P. Pareja, M. Mercy, J.C. Gachon, A. Amariglio and H. Amariglio, Ind. Eng. Chem. Res. 38 (1999) 1163.
[17] L. Guczi, L. Borko, Zs. Koppany and F. Mizukami, Catal. Lett. 54 (1998) 33.
[18] M. Belgued, P. Pareja, A. Amarigalio and H. Amarigalio, Nature 352 (1991) 789.
[19] M. Belgued, A. Amariglio, P. Pareja and H. Amariglio, J. Catal. 159 (1996) 441.
[20] M. Belgued, A. Amariglio, P. Pareja and H. Amariglio, J. Catal. 161 (1996) 282.
[21] M.C. Wu and D.W. Goodman, J. Am. Chem. Soc. 116 (1994) 1364.
[22] F. Solymosi, A. Erdohelyi, J. Cserenyi and A. Felvegi, Catal. Lett. 16 (1992) 399.
[23] F. Solymosi, A. Erdohelyi, J. Cserenyi and A. Felvegi, J. Catal. 147 (1994) 272.
[24] L. Guczi, K.V. Sharma and L. Borko, J. Catal. 167 (1997) 495.
[25] L. Guczi, K.V. Sharma and L. Borko, Catal. Lett. 39 (1996) 43.
[26] M.M. Koranne, D.W. Goodman and G.W. Zajac, Catal. Lett. 30 (1995) 219.
[27] J.N. Carstens and A.T. Bell, J. Catal. 161 (1996) 423.
[28] D.J. Trevor, D.M. Cox and A. Kaldor, J. Am. Chem. Soc. 112 (1990) 3742.
[29] S. Brunauer, P.H. Emmett and E. Teller, J. Am. Chem. Soc. 60 (1938) 309.
[30] Dollimore and G.R. Heal, J. Colloid Interface Sci. 33 (1970) 508.
[31] S. Brunauer, L.S. Deming, W.S. Deming and E. Teller, J. Am. Chem. Soc. 62 (1940) 1723.
[32] K.S.W. Sing, Chem. Ind. (1968) 1520
[33] B.C. Lippens and J.H. de Boer, J. Catal. 4 (1965) 319.
[34] K.E. Coulter and A.G. Sault, J. Catal. 154 (1995) 56.
[35] M.P. Rosynek and C.A. Polansky, Appl. Catal. 73 (1991) 97.
[36] R. Reuel and C.H. Bartholomew, J. Catal. 85 (1984) 63.
[37] J.S.M. Zadeh and K.J. Smith, J. Catal. 176 (1998) 115.
[38] E. Mielczarski, S. Monteverdi, A. Amariglio and H. Amariglio, Appl. Catal. A 104 (1993) 215.
[39] T. Koerts and R.A. van Santen, J. Chem. Soc. Chem. Commun. (1991) 1281.
[40] T. Koerts, P.A. Leclercq and R.A. van Santen, J. Am. Chem. Soc. 114 (1992) 7272.
[41] Marceau, J.M. Tatibouet, M. Che and J.S. Just, J. Catal. 183 (1999) 384.
[42] T.M. Duncan, P. Winslow and A.T. Bell, J. Catal. 93 (1985) 1.
[43] T.M. Duncan, J.A. Reimer, P. Winslow and A.T. Bell, J. Catal. 95 (1985) 305.